*J. Fluid Mech.* (1986), *vol.* 173, *pp.* 191–205
*Printed in Great Britain*



# Individual and collective fluid dynamics of swimming cells

By JOHN O. KESSLER
Physics Department, University of Arizona, Tucson, AZ 85721, USA

(Received 22 May 1986)

Gravitational and viscous torques acting on swimming micro-organisms orient their trajectories. The horizontal component of the swimming velocity of individuals of the many algal genera having a centre of mass displaced toward the rear of the cell is therefore in the direction $\boldsymbol{g} \times (\nabla \times \boldsymbol{u})$, where $\boldsymbol{g}$ is the acceleration due to gravity. This phenomenon, called gyrotaxis, results in the cells swimming toward downward-flowing regions of their environment. Since the cells' density is greater than that of water, regions of high (low) cell concentration sink (rise). The horizontal component of gyrotaxis reinforces this type of buoyant convection, whilst the vertical one maintains it. Gyrotactic buoyant convection results in the spontaneous generation of descending plumes containing high cell concentration, in spatially regular concentration/convection patterns, and in the perturbation of initially well-defined flow fields. This paper presents a height- and azimuth-independent steady-state solution of the Navier–Stokes and cell conservation equations. This solution, and the growth rate of a concentration fluctuation, are shown to be governed by a parameter similar to a Rayleigh number.

## 1. Introduction

The swimming of micro-organisms comprises two aspects: propulsion and orientation. G. I. Taylor's paper of 1951 was the first to consider the fluid dynamics of propulsion. This paper is concerned with the orientation of the cells' trajectories by one or more torques applied to the cell bodies, and with the resultant individual and collective phenomena. Swimming micro-organisms progress along trajectories whose geometry depends on the way in which the swimmers control their propulsive apparatus and on torques which orient their bodies. When the distribution of mass within an organism is asymmetric, so that its centres of gravity and buoyancy do not coincide (figure 1), gravity provides a torque which tends to maintain the organism's axis vertical. Gradients of the velocity of the fluid within which the organism swims result in a viscous torque. In a neutral environment, when the gravitational and viscous torques compensate, they determine the orientation of the swimmer and therefore its trajectory, since the direction of locomotion is determined by its axis. A neutral environment is one which does not stimulate a micro-organism's senses or alter its metabolism.

Micro-organisms may seek to accumulate in or depart from regions of their environment that are distinguished by spatial variations of stimuli, such as chemical concentration, light intensity, or direction of illumination. Such behaviour, which requires interaction of organism and stimulus and generally seems purposeful, has been investigated since the middle of the last century. A complex categorization (Diehn *et al.* 1977) that describes various sensing modes and stimulus–response

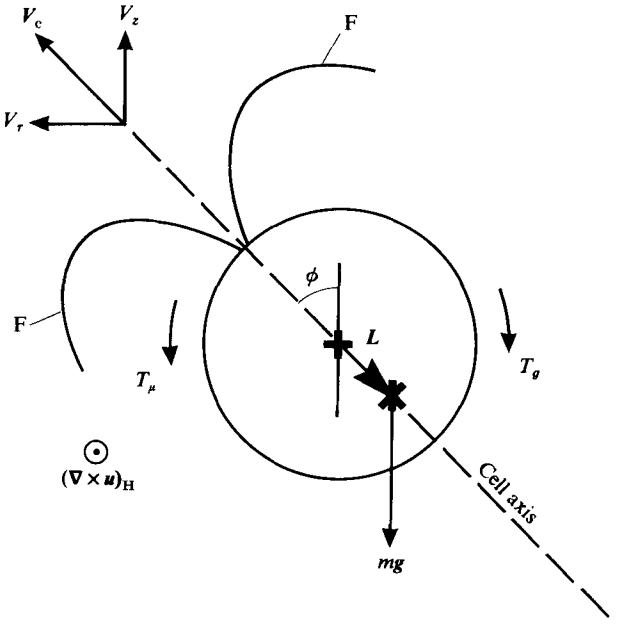


FIGURE 1. Orientation of the swimming velocity $V_c$ of an algal cell idealized as a sphere. $L$ is the rearward displacement of the centre of mass (*) relative to the geometrical centre (+). As in (2), the gravitational torque $T_g = mgL \sin\theta$ is balanced by the viscous torque $T_\mu = 4\pi\mu a^3(\nabla \times u)_H$, where $(\nabla \times u)_H$ is the horizontal component of vorticity. The cells swim in the direction $-(L/L)$, propelled by their flagella F.

sequences has been developed. In the simplest version, stimulus-guided locomotion is called a 'taxis'. For example, swimming toward (away) from a light source is positive (negative) phototaxis. Swimming along a chemical concentration gradient is chemotaxis.

Physically determined taxes (Kessler 1986) arise from torques that orient swimming cells. Thus, upswimming, or negative geotaxis, can be due to gravitational torque or to a combination of viscous and gravitational torques (Roberts 1981). Compensating viscous and gravitational torques produce gyrotaxis (Kessler 1984).

Negative geotaxis results in up-accumulation of cell populations. Gyrotaxis guides swimming cells horizontally, away from upwelling and toward downwelling regions of fluid. Since the density of the swimmers is greater than that of their embedding medium, accumulative behaviour results in buoyant convection. A situation similar to Bénard convection, due to upswimming, has been discussed by Childress, Lavandowsky & Spiegel (1975). Since gyrotaxis guides cells laterally into descending regions of fluid (Kessler 1985*a*, *b*), it reinforces population fluctuations. These collective effects are modified by the cells' ever-present random locomotion, which can to a first approximation be modelled by diffusion. This paper discusses the collective phenomena just introduced. It also reviews the gyrotactic generation of hydrodynamically focused beams of cells.

## 2. Cell characteristics

The micro-organisms considered here are single cells of swimming algae. Although their shape is approximately ellipsoidal, in many cases it is almost spherical, and that shape will be assumed here. They vary in diameter from 0.4 to $4 \times 10^{-3}$ cm, are

| Symbol | Name | Range | Estimated value used in calculations |
|---|---|---|---|
| | | Cell properties | |
| $\rho_c$ | Density | 1.01–1.10 | 1.05 gm cm$^{-3}$ |
| $\Delta\rho/\rho$ | Specific gravity | 0.01–0.10 | 0.05 |
| $a$ | Average radius | $2\times10^{-4}$–$2\times10^{-3}$ | $5\times10^{-4}$ cm |
| $v$ | Volume per cell | $3\times10^{-11}$–$3\times10^{-8}$ | $5\times10^{-10}$ cm$^3$ |
| $V_c$ | Swimming speed | 0–$2\times10^{-2}$ | $10^{-2}$ cm s$^{-1}$ |
| $L$ | Centre of gravity offset | 0–0.1$a$ | $10^{-5}$ cm |
| $D$ | Diffusivity of cells | $5\times10^{-5}$–$5\times10^{-3}$ | $5\times10^{-4}$ cm$^2$ s$^{-1}$ |
| $n$ | Concentration | 0–$1/v$ | |
| $n_0$ | Typical background | 0–$10^7$ | $10^6$ cells cm$^{-3}$ |
| $\mu$ (or $\mu/\rho=\nu$) | Viscosity | $10^{-2}$ | $10^{-2}$ gm cm$^{-1}$ s$^{-1}$ (cm$^2$ s$^{-1}$) |
| | | Combination properties | |
| $\beta$ | Gyrotactic length (for a sphere $C=3$) | $C\mu V_c/gL\rho_c$ | $5\times10^{-2}$ cm |
| $\alpha$ | Fluid velocity/cell concentration coupling | $(\Delta\rho/\rho)gv/\nu$ | $2.5\times10^{-6}$ cm$^2$ s$^{-1}$ |
| $1/\tau_g$ | Growth/recruitment rate | $\alpha\beta n_0$ | 0.13 s$^{-1}$ |
| $G$ | Gyrotactic Rayleigh number ($\lambda$ is a radial dimension in cm) | $\frac{(\Delta\rho/\rho)vn_0\beta\lambda^2}{\nu D}$ | $250\lambda^2$ [1] |
| $\gamma n_0$ | Radius scale for self-focusing | $\frac{(\Delta\rho/\rho)vn_0\beta}{8\nu D}$ | $1/0.17^2$ cm$^{-2}$ |

TABLE 1. Definitions and magnitude of parameters. The parameter ranges are derived from observations, from the literature, and by guessing. The numerical values in the last column apply approximately ($\pm50\%$ ?) to a favourite test organism, *Chlamydomonas nivalis*. The value of $D$ is a pure guess, based on collision mean-free paths ($D\approx V_c/12\pi a^2 n$), where $n$ is 2 or 3 times $n_0$, or average distance $\delta$ covered by swimming cells between radical changes in direction ($D\approx\frac{1}{3}V_c\delta$). Observation indicates that $\delta\approx100a$. The significance of $\lambda$ depends upon circumstances.

equipped with two or four flagella of length a body diameter or greater, and they swim forward by means of breaststroke-like motions (Nultsch 1983). Their centre of gravity is displaced rearward, relative to their geometric centre. As a result, dead cells tend to be suspended with their flagella oriented upward and, on average, live cells swim upwards. The density of cells is approximately 5% greater than water. They swim at speeds $V_c$ up to $2\times10^{-2}$ cm s$^{-1}$, the average being $0.5$–$1.0\times10^{-2}$ cm s$^{-1}$. The cell Reynolds number is therefore very much less than 1. Typical genus names are *Chlamydomonas*, *Carteria*, and *Dunaliella*, a salt-water type. A summary of characteristics and nomenclature is given in table 1.

## 3. Gyrotaxis

The viscous torque on a sphere of radius $a$ in a fluid of viscosity $\mu$ is given by

$$\boldsymbol{T}=4\pi\mu a^3(\boldsymbol{\nabla}\times\boldsymbol{u}-2\boldsymbol{\Omega}), \tag{1}$$

where $\boldsymbol{u}$ is the fluid velocity field and $\boldsymbol{\Omega}$ the sphere's angular velocity. The gravitational torque on a sphere whose centre of mass is displaced by $\boldsymbol{L}$ from its geometric centre is $m\boldsymbol{L}\times\boldsymbol{g}$; the sphere's mass is $m$, and $\boldsymbol{g}$ is the acceleration due to gravity. For algal cells of the type considered, $\boldsymbol{L}$ is a few percent of the cell radius.

The offset is caused by the posterior location of organelles, such as the chloroplast. Steady orientation of the sphere axis $\boldsymbol{L}$ is specified by

$$m\boldsymbol{L}\times\boldsymbol{g}+4\pi\mu a^3\boldsymbol{\nabla}\times\boldsymbol{u}=0, \tag{2}$$

given $\boldsymbol{\nabla}\times\boldsymbol{u}$.

Cells of the type considered here swim forward with velocity $\boldsymbol{V}=-(\boldsymbol{L}/L)\,V_c$. When $\boldsymbol{u}=w(r)\,\hat{z}$, where $r$ is the radial coordinate in cylindrical polar coordinates, $\hat{z}$ is an upward unit vector, and $\boldsymbol{V}=V_r\hat{r}+V_z\hat{z}$,

$$V_r=-\frac{4\pi\mu a^3}{mgL}\frac{\mathrm{d}w}{\mathrm{d}r}\equiv-\beta\frac{\mathrm{d}w}{\mathrm{d}r}. \tag{3}$$

The length $\beta$ summarizes a cell's gyrotactic behaviour within a single parameter. Equation (3) assumes the stable configuration (Kessler 1985*b*, 1986), where the centre of mass lies below the centre of the cell.

This paper considers only the radial component of gyrotaxis, given by (3). The $(z,\phi)$-dependence will be suppressed. This assumption allows the derivation of relatively simple basic results which bear on the radially symmetric accumulation of cells into tall descending columns, either in prescribed flows, or in flows generated by buoyant convection. Although it permits an estimate of the steady-state spacing of concentration/convection patterns, it eliminates the possibility of obtaining a detailed description of their geometry, or of the role of upward swimming in maintaining the patterns.

Equation (3) states that cells swim toward the axis of a vertically downward cylindrical Poiseuille flow, $w(r)=-w(0)\,(1-r^2/R^2)$, and toward the periphery of an upward one, as discussed in Kessler (1985*b*), and rather in contrast to the diffusive dispersion of passive solutes (Taylor 1953) or radial accumulation of inert particles (Happel & Brenner 1965). The equation for the cell concentration $n(r,z)$ is also contained in Kessler (1985*b*). The radial component of the trajectory in the downward Poiseuille flow is given by

$$\frac{\mathrm{d}r}{\mathrm{d}t}=-\frac{2\beta w(0)\,r}{R^2},$$

or

$$r=r_0\,\mathrm{e}^{-2\beta w(0)t/R^2}. \tag{4}$$

The time constant $R^2/2\beta w(0)\approx 25$ s for $R\approx 0.5$ cm, $\beta=5\times10^{-2}$ cm (table 1) and $w(0)\approx 0.1$ cm s$^{-1}$. Figure 2 shows a beam of swimming cells. The generation of the beam is shown in Kessler (1985*b*, figures 2, 3 and 4). Outward focusing in an upflow is also shown in that paper (figure 6) and in Kessler (1985*a*).

Random swimming is superimposed upon gyrotaxis. Although its characteristics are not well understood, the conventional modelling is by diffusion. The radial cell flux $j$ is then given by

$$j=nV_r-D\frac{\partial n}{\partial r}, \tag{5}$$

where $n$ is the cell concentration and $D$ the diffusivity. One may guess the magnitude of $D$ by watching cells through a microscope. One finds that typical algal cells tend to swim 'straight' about 50–100 body lengths between substantial changes of direction. Then $D\approx\text{const}\,V_c\,a$, or $D\approx5\times10^{-4}$ cm$^2$ s$^{-1}$. If collisions dominate change of direction, $D\approx V_c/3n\sigma$, where $\sigma$ is a collision cross-section (cm$^2$). In a typical axially focused beam of cells, the guessed magnitudes of these rather differently obtained diffusivities is similar.

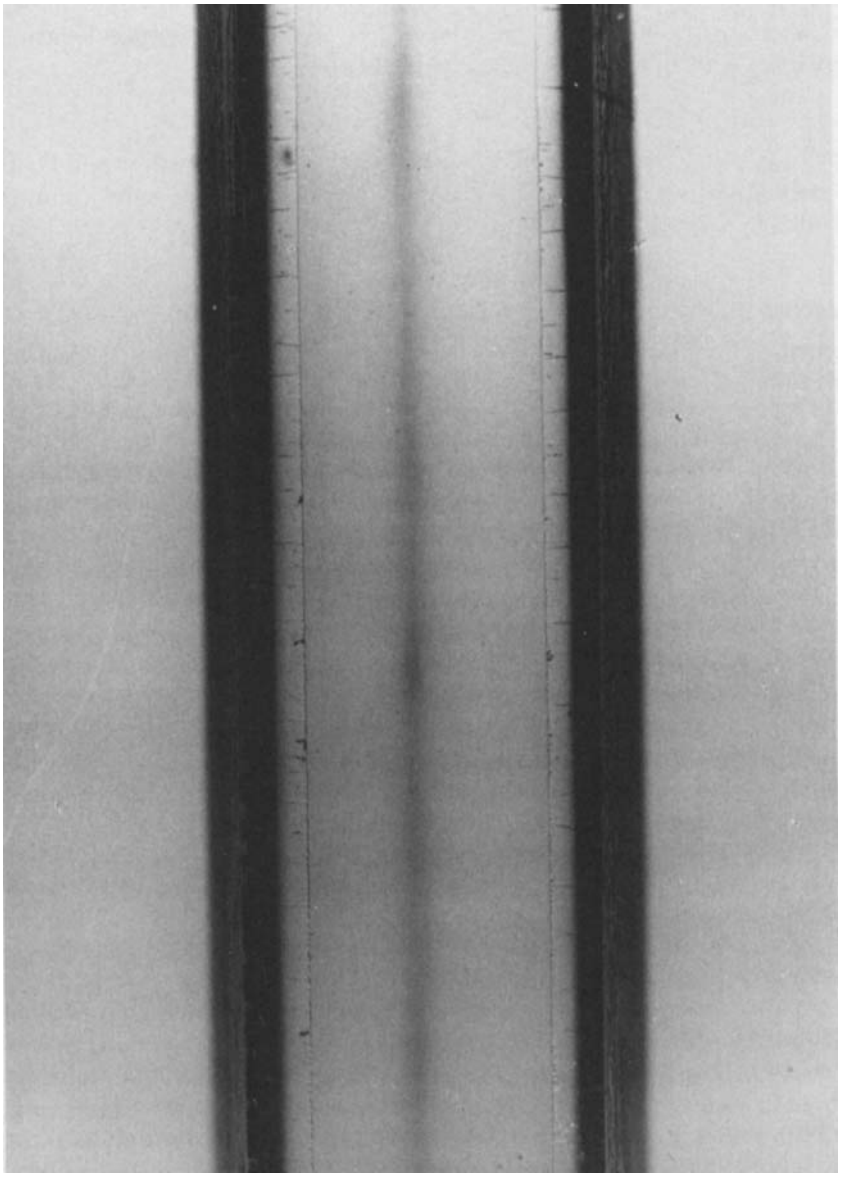

FIGURE 2. Focused beam of cells. Fluid containing the swimming algae *Chlamydomonas nivalis* flows slowly (centre velocity $\approx 0.1$ cm s$^{-1}$) down a cylindrical tube with a flat front 8 cm across. The beam of cells is produced by gyrotaxis and broadened by diffusion.

The cell conservation equation is

$$\frac{\partial n}{\partial t} + \boldsymbol{u} \cdot \boldsymbol{\nabla} n = -\frac{1}{r} \frac{\partial}{\partial r} rj. \tag{6}$$

The $\boldsymbol{u} \cdot \boldsymbol{\nabla} n$ term vanishes when $\boldsymbol{u} = \hat{z} w(r, t)$ and $n = n(r)$. For steady state,

$$j = -\beta n \frac{\mathrm{d}w}{\mathrm{d}r} - D \frac{\mathrm{d}n}{\mathrm{d}r} = 0, \tag{7}$$

or
$$n = n_0\, e^{-(\beta/D)(w-w_0)}, \tag{8}$$

where $n_0$ and $w_0$ are constants pertaining to the same reference location. When $w(r) = -w(0)(1-r^2/R^2)$, $w_0 = -w(0)$ and $n_0 = n(0)$,

$$n = n(0)\, \mathrm{e}^{-\beta w(0) r^2/DR^2}. \tag{9}$$

This distribution has been (approximately) observed by the author and G. J. Morris, using a segmented collector at the bottom of the focusing tube (manuscript in preparation). It is qualitatively indicated by figure 2.

## 4. Collective phenomena

The density of a fluid containing a concentration of $n$ cells cm$^{-3}$, each of volume $v$ and density $\rho_c$, is

$$\rho = \Delta\rho n v + \rho_w, \tag{10}$$

where $\rho_w$ is the density of water and $\Delta\rho = \rho_c - \rho_w$. When cells accumulate in a fluid region, its density increases relative to surrounding regions. When a cylindrical downward flow produces a beam of cells (equation (8)) near the axis, the weight of that high-cell-concentration region generates a downward buoyant convection velocity which adds to the initial Poiseuille flow. If the flow rate $2\pi Q$ is kept constant, the buoyant component generates a pressure gradient which results in a peripheral upward velocity of the fluid such that $\int_0^R w(r)\, r\, \mathrm{d}r = Q$. It is observed that when the focusing Poiseuille flow is stopped the cell beam, which is approximately Gaussian (equation (9)), remains, continues to sink and appears to accumulate more cells. Thus the buoyant convection and associated pressure gradient continue, trapping the cells located in the region where $\mathrm{d}w/\mathrm{d}r > 0$. These cells swim toward the axis, where they increase the mass and therefore the downward convection, the pressure gradient and the vorticity. Such 'green holes' are somewhat analogous to black holes, since (i) the 'attraction' of cells toward the axis is proportional to the weight of cells already in its vicinity, (ii) there is a limiting radius, where $\mathrm{d}w/\mathrm{d}r = 0$, beyond which the cells move outward, and (iii) a singularity develops at $r = 0$, as will be shown.

The generation of self-focused cell streamers can also occur spontaneously. Local fluctuations in cell concentrations sink, thereby generating a fluid velocity field which accumulates more cells. For that reason, initially well-mixed cell cultures containing $n_0 \gtrsim 10^6$ cells cm$^{-3}$ tend to break up into downward-convecting columns containing higher than average cell concentrations, separated by upward-convecting regions containing few cells (Kessler 1986) and figure 3. This effect occurs even in very tall vessels (Kessler 1985*b*), far below the upper surface of the fluid. This fact implies that the density gradient which develops near the top of a fluid containing upward-swimming heavy cells is not required to initiate buoyant convection. Typical times for the initial appearance of visible streamers are 10–30 s.

A concentrated cell culture of low aspect ratio (height/width) tends to generate regular patterns of cell concentration and fluid convection, partly because of negative geotaxis (Childress *et al.* 1975) and partly owing to gyrotaxis. Several examples are shown in Kessler (1985*b*, 1986). Such patterns may be thought of as an array of many coexisting self-focused streamers. When the cells entrained in downwelling fluid arrive at the bottom of the vessel, they are advected upward in the low concentration, slowly upwelling return fluid, and they also swim upward until they are refocused into a downward-streaming column. The downward columns, or streamers, eventually arrange themselves in a regular array. When the fluid layer containing the cells

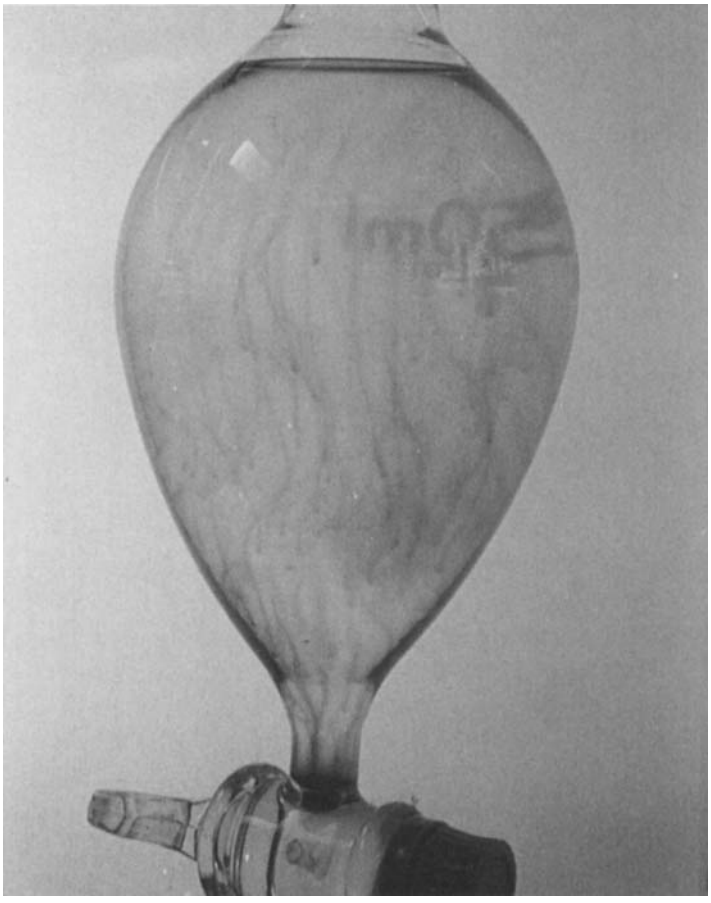

FIGURE 3. Spontaneous breakup of an initially well-stirred algal cell culture. The dark streaks are self-focused descending regions containing a higher concentration of cells than the intervening fluid. Nucleation appears to have been fairly random throughout the vessel – but note the absence of streamers near the upper interface. Their sinuous character may be due to motions of the fluid remaining from stirring, or to temperature-gradient-driven convection. Time after stirring: approximately 5 min.

is deeper than 1–2 cm, this array, observed horizontally, is visible only near the bottom of the container. The steady-state theory presented below provides an estimate of the column spacing. This estimate must eventually be corrected by including $(z, \phi)$-dependences.

It is generally observed that any individual long column of gyrotactically focused cells tends to develop blips, localized regions of high cell concentration, which grow, and of course sink faster than the focused beam. This phenomenon occurs when $n_0$, the background concentration, is 'high'. In a vertical cylindrical focusing tube, the effect is reduced when there is a net downward flow $2\pi Q$, and enhanced when $Q = 0$, i.e. when the entire velocity field is due to the sinking cell column.

The effect is shown in figure 4 at an early stage, superimposed on a cell beam focused in a downflow. When $Q$ is set equal to zero, the blips eventually develop into beautiful thermal-like structures, attached to a vortex ring (figure 5). Isolated streamers descending in a wide bottle also generate the same effect (figure 6).

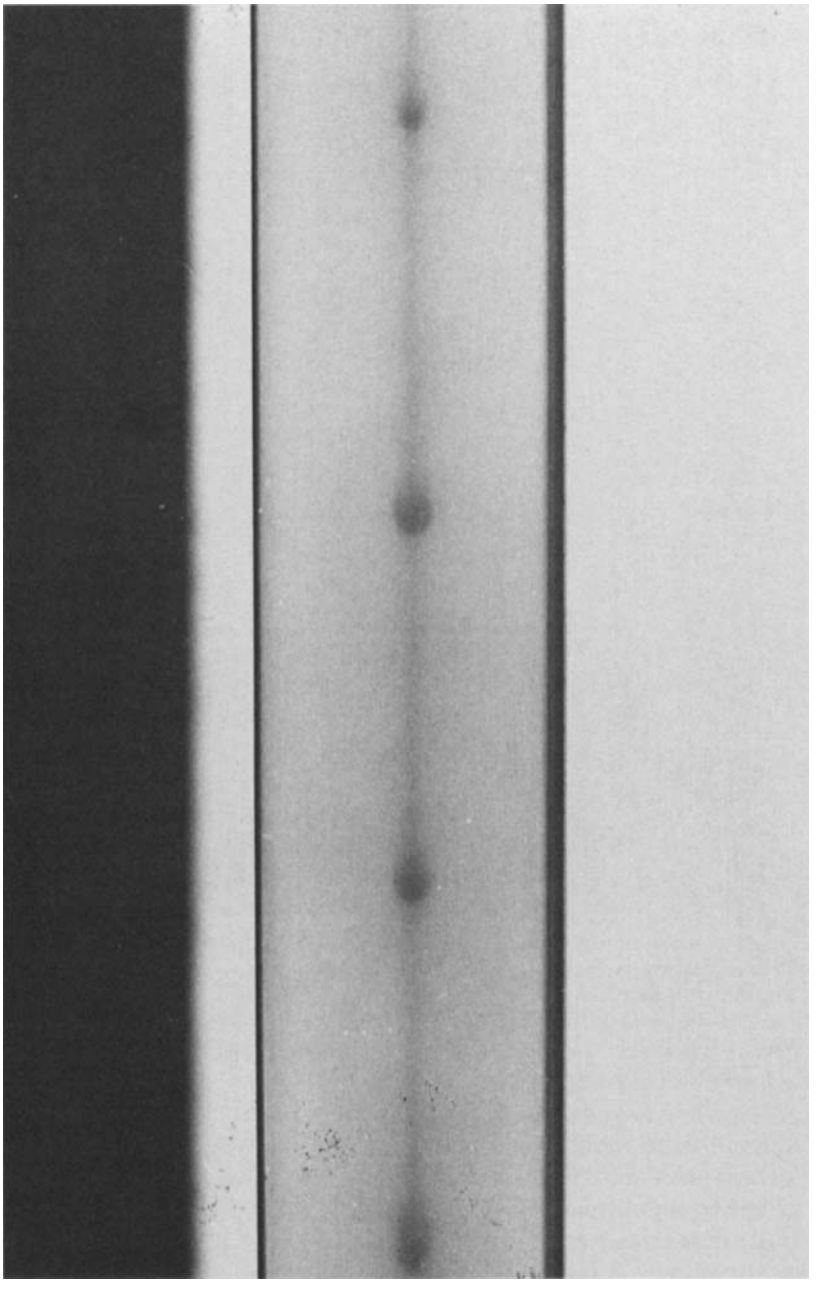

FIGURE 4. Spontaneous formation of high concentration regions on a gyrotactically focused algal beam. The diameter of the cylindrical tube is 1.3 cm. The central streak is the focused beam, and the superimposed bulbous expansions are growing 'blips'. The central velocity of the focusing downward Poiseuille flow is $u_0 \approx 0.1$ cm s$^{-1}$. The (unknown) actual central flow velocity is more rapid because of the weight of the beam. The blips sink with velocity $2u_0$–$5u_0$.

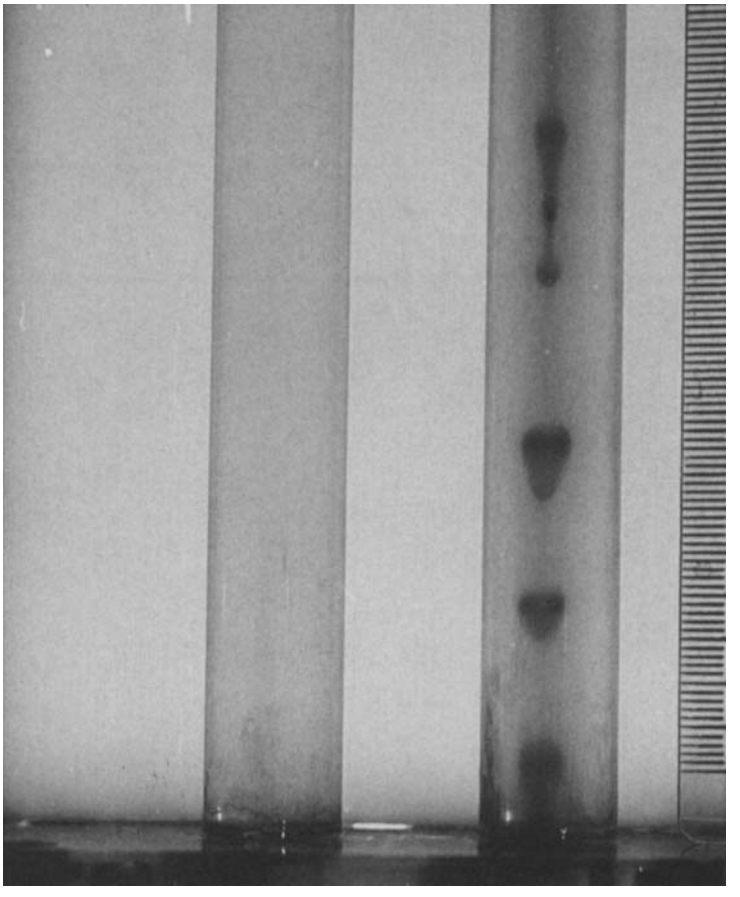

FIGURE 5. Blip instability at a late stage. The blips from figure 4 have grown into a structure having a toroidally circulating rear section. Upper blips sometimes catch lower ones and amalgamate with them. Near the top, the central (darkest) blip has just passed through the preceding one, distorting it. The scale is in mm.

### 4.1. *Steady state*

The Navier–Stokes equation for the velocity $\boldsymbol{w}(r) = \hat{z}w(r)$ of a steady, slow viscous flow of fluid containing $n(r)$ cells cm$^{-3}$ is

$$\frac{1}{r}\frac{\mathrm{d}}{\mathrm{d}r}r\frac{\mathrm{d}w}{\mathrm{d}r} = \alpha n(r) + \frac{p_z}{\mu}, \tag{11}$$

where the cell-concentration/fluid-velocity coupling constant $\alpha = (\Delta\rho/\rho)\,vg/\nu$, $\mu$ is the viscosity, $\nu = \mu/\bar{\rho}$ and the vertical pressure gradient $p_z$ includes $\bar{\rho}g$, where $\bar{\rho}$ is the average fluid density. The $(z, \phi)$-dependence has been suppressed in order to facilitate finding a solution, and in approximate conformity with a wide range of experimental conditions. The pressure gradient can be inferred from the condition $\int_0^R w(r)\,r\,\mathrm{d}r = Q$, where $2\pi Q$ is a prescribed flow rate and $R$ is the radius of the container. The solution must satisfy $w(0)$ finite, $w(R) = 0$, $\mathrm{d}w/\mathrm{d}r = 0$ at $r = 0$, and conservation of cells, $\int_0^R n(r)\,r\,\mathrm{d}r = \frac{1}{2}R^2 n_0$, where $n_0$ is the initially uniform background concentration. No vertical cell-flux condition is imposed for this $z$-independent

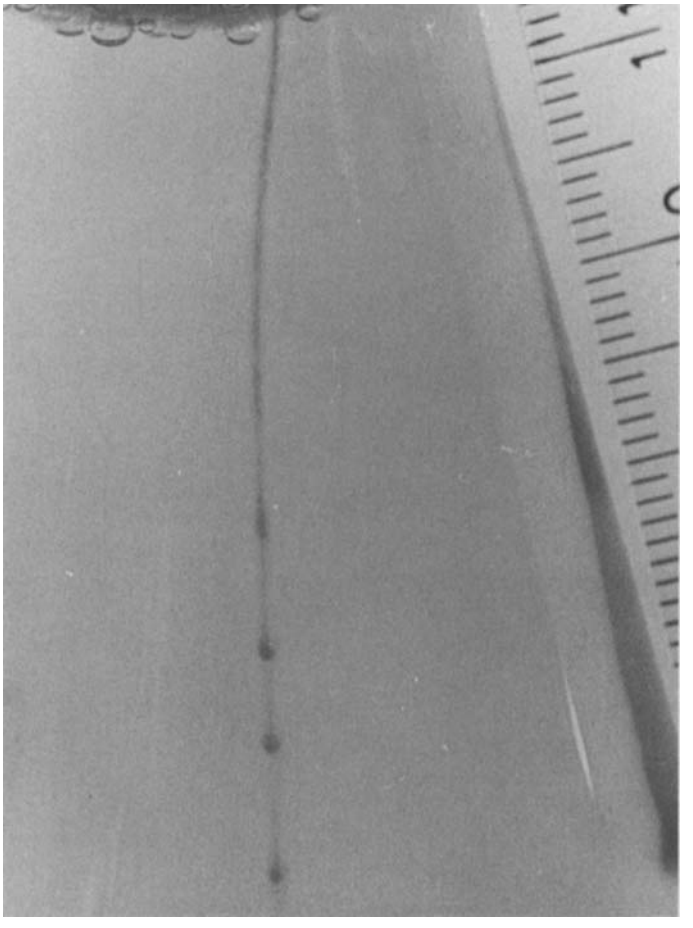

FIGURE 6. Blips in a wide container. A stream of cells emerges from a leak in a cotton-wool plug at the top of an erlenmyer flask. Unlike passive plumes, the beam narrows, due to gyrotaxis, and spontaneously forms blips, even in this situation where the outer surface is remote, see also Kessler (1986), figure 12.

situation. The cell concentration $n(r)$ is given by (8). Equations (7) and (8) imply that the radial cell flux vanishes at all $r \leqslant R$.

When $\alpha n(r) \ll p_z/\mu$, the solution of (11) is Poiseuille flow, with $n(r)$ then given by (10), $w(0)$ being determined from $Q$. In general, inserting $n(r)$ from (8) into (11) gives

$$-\frac{1}{r}\frac{\mathrm{d}}{\mathrm{d}r}\, r \frac{\mathrm{d}}{\mathrm{d}r} \log n = \frac{\alpha\beta}{D}\, n + \frac{\beta}{D\mu}\, p_z. \tag{12}$$

A suitable closed-form solution for (12) and subsidiary conditions can be found when $p_z = 0$. This extra condition can be met exactly by the proper experimental choice of $Q$, and approximately automatically when $R$ becomes very large.

One set of generic solutions of (12) is given by

$$n(r) = Ar^{-2} \cosh^{-2}(B + C \log r), \tag{13}$$

where $A, B, C$ are arbitrary constants. The present context requires $n(0)$ to be finite and $n(\infty) \to 0$. Then $C = 1$ and

$$n(r) = \frac{n(0)}{(1+\gamma n(0)\, r^2)^2}, \tag{14}$$

where $\gamma = \alpha\beta/8D$. A general discussion of other solutions of (12), with $p_z = 0$, may be found in Joseph & Lundgren (1973). Equation (12) also appears in Childress & Percus (1981), in the context of chemotaxis, where the concentration of chemical attractant replaces $w(r)$. The central concentration $n(0)$, should be found from cell number conservation, i.e.

$$\int_0^R n(r)\, r\, \mathrm{d}r = \tfrac{1}{2} n_0 R^2, \tag{15}$$

or

$$\frac{n(0)\, R^2}{1+\gamma n(0)\, R^2} = n_0 R^2. \tag{16}$$

It appears that when $\gamma n(0)\, R^2 \gg 1$, $n_0 = 1/\gamma$, which is nonsense, since $\gamma$ characterizes the properties of the individual cells and of the fluid and has nothing to do with cell concentration! If one returns to (15) and integrates to an intermediate radius $R_1 < R$,

$$\frac{n(0)}{1+\gamma n(0)\, R_1^2} = n_1, \tag{17}$$

where $n_1$ is the average concentration for $0 < r \leqslant R_1$. Inverting (17), one finds that

$$n(0) = \frac{n_1}{1-\gamma n_1 R_1^2}. \tag{18}$$

It is now evident that $n(0)$ blows up when $\gamma n_1 R_1^2 \to 1$. For larger values of $\gamma n_1 R_1^2$, (14) is no longer a valid solution. Since $n_1 \geqslant n_0$, one may consider $\pi R_1^2 = \pi/\gamma n_0$ to be the maximum area over which cells can collect themselves into a steady columnar solution of (12) (with $p_z = 0$). The limited capacity of the solution given by (14) arises from the fact that its width as well as its height is related to $n(0)$.

There are two ways of considering a container having radial dimension $R \gg R_1$:

(*a*) Steady state. Many replicas of the gyrotactic columns described by (14) can be set up in such a container. Since the symmetric radial dependence of the solution has short range, one may suppose that the interference between neighbouring columns will not change the basic properties of the solution. The total area of $N$ columns approximately equals the area of the container, i.e. $N\pi/\gamma n_0 \approx \pi R^2$. For a square pattern, which occurs sometimes (Kessler 1985*b*), $N \approx \pi R^2/l^2$, where $l$ is the mean column spacing. Thus $l^2 \approx 1/\gamma n_0$. For the values given in table 1, $l \approx 0.17$ cm for $n_0 = 10^6$, which closely matches observation. It should be realized, however, that this calculation must be corrected by the inclusion of cell flux conservation, total fluid flow conservation, $(z, \phi)$-dependence, and proper matching.

(*b*) Unsteady case. If one arranges for the presence of only a single axial column of cells, e.g. by starting one with Poiseuille flow focusing, the velocity field of the sinking column continues to attract cells toward the axis even when the $n_0 \gamma R^2 = 1$ limit is exceeded. Since these cells cannot be accommodated into the steady solution, an intrinsically time-dependent mode must arise. It seems very likely that the blips (figures 3–5) which are $(t, z)$-dependent structures originate in this way.

The velocity field of the steady solution is found by combining (8) and (14) and the boundary conditions. It is

$$w(r) = \frac{2D}{\beta} \log \frac{(1+\gamma n(0)\, r^2)}{(1+\gamma n(0)\, R^2)}. \tag{19}$$

At large $r$, $w(r)$ is approximately proportional to $\log r$ even when the core is unsteady. This dependence corresponds to a laminar cylindrical flow driven by a thin, heavy immiscible axial column of fluid sedimenting within lighter fluid contained in a cylindrical enclosure. The velocity scale $D/\beta$ must then be replaced by a factor proportional to the density of the sedimenting column. In any event, the dependence of $\mathrm{d}w/\mathrm{d}r$ on $1/r$ causes an inward flux of cells, as shown by (3) and (5).

Inserting the normalization condition, (18), with $R_1 = R$ and $n_1 = n_0$ into (19), one obtains

$$w(r) = \frac{2D}{\beta} \log [1 + n_0 \gamma (r^2 - R^2)]. \tag{20}$$

The condition $n_0 \gamma R^2 < 1$ is again required, to maintain a finite value for $w(0)$.

## 5. Growth or decay of concentration fluctuations

Consider a cell culture initially having uniform cell concentration $n_0$ and fluid velocity $w(r) = 0$. According to (11), a fluctuation in concentration, $n_\mathrm{f}(r, t)$ produces a fluctuation in $w(r)$, which tends to reinforce the concentration fluctuation. The cells' random swimming, or diffusion, tends to disperse the fluctuation. Fluctuations can spontaneously result from the cells' random swimming, or they may be caused 'externally' by fluid motions or non-uniform illumination.

Assuming only $r$-dependence, the growth or decay of a fluctuation is governed by cell conservation. Equation (6) now reads

$$\frac{\partial n_\mathrm{f}}{\partial t} = \frac{1}{r} \frac{\partial}{\partial r} r \left[ (n_0 + n_\mathrm{f}) \beta \frac{\partial u}{\partial r} + D \frac{\partial n_\mathrm{f}}{\partial r} \right]. \tag{21}$$

For quasi-steady conditions and $p_z = -(\alpha \mu n_0 + \rho_\mathrm{w} g)$, (11) gives

$$r \frac{\partial w}{\partial r} = \alpha \int_0^r n_\mathrm{f}(r', t)\, r'\, \mathrm{d}r'.$$

Changes in $p_z$ can be ignored when the containing vessel's radius is much larger than that of the fluctuation.

The linear approximation for growth of a perturbation can be obtained by setting $n_\mathrm{f}(r, t) = n_1(t) f(r)$ and assuming that $n_1(t)/n_0 \ll 1$. Equation (21) then yields $f(r) = J_0(r/\lambda)$ and $n_1(t) = n_1(0) \exp(t/\tau)$, where $J_0$ is the Bessel function of zero order. The choice of a solution which has a finite maximum at $r = 0$ and a decreasing value at large $r$ requires $\lambda^2 > 0$. The value of $\lambda$ is determined by particle conservation, to give $\lambda_\nu^{-1} = j_1^\nu / R$, where $j_1^\nu$ is the $\nu$th root of $J_1$, and $R$ is either the radius of the container or the (artificially chosen) radius of the perturbation. This solution also demands that $1/\tau = \alpha\beta n_0 - D/\lambda^2$. Thus the perturbation grows when $\alpha\beta n_0 \lambda^2 / D > 1$. This linear solution can be used to estimate the nonlinear dependence. Setting $n_\mathrm{f}(r, t) = n_1(t) J_0[r/\lambda(t)]$ and expanding the result to order $(r/\lambda)^2$, one obtains

$$\left(\frac{r}{\lambda}\right)^0 : \quad \frac{\mathrm{d} \log n_1}{\mathrm{d}t} = \alpha\beta(n_0 + n_1) - \frac{D}{\lambda^2} \tag{22}$$

and

$$\left(\frac{r}{\lambda}\right)^2 : \quad \frac{\mathrm{d} \log \lambda}{\mathrm{d}t} = -\alpha\beta n_1. \tag{23}$$

These equations indicate the growth of $n_1(t)$ and imply narrowing. However, if $\lambda$ is chosen by a fixed boundary condition, it may not change, and (23) is simply an indication that in a proper normal-mode expansion,

$$n_f(r,t) = \sum_\nu C_\nu \, e^{t/\tau_\nu} J_0(r/\lambda_\nu),$$

the trend would be toward narrowing.

If the nonlinear expansion is begun with a Gaussian perturbation, $n_f = n_1(t) \exp -[r/\lambda(t)]^2$, the width is summarized by $\lambda(t)$. Such a perturbation could be obtained experimentally by a short interval of Poiseuille flow. In that case, expanding to $r^2/\lambda^2$, one obtains

$$\frac{\mathrm{d} \log n_1}{\mathrm{d}t} = \alpha\beta(n_0+n_1) - \frac{4D}{\lambda^2} \tag{24}$$

and

$$\frac{\mathrm{d}\lambda^2}{\mathrm{d}t} = -2\alpha\beta n_1 + 4D. \tag{25}$$

This set is very similar to (22) and (23) but it also includes the diffusive broadening of the width when there is no gyrotactic narrowing. Then,

$$n_1 \approx \frac{n_1(0)\, e^{t/\tau}}{1+n_1(0)\,\alpha\beta\tau(1-e^{t/\tau})}, \tag{26}$$

where $1/\tau \approx \alpha\beta n_0 - 4D/\lambda_0^2$. For $t/\tau \to 0$,

$$n_1 \approx n_1(0)\left\{1+\alpha\beta t[n_0+n_1(0)] - \frac{4Dt}{\lambda_0^2}\right\}. \tag{27}$$

Analysis of long-time growth requires the exact normal-mode expansion in Bessel functions.

In the limit of vanishingly small initial perturbation amplitude $n_1(0)$, the amplitude $n_1(t)$ changes at the rate $\tau^{-1} = (\alpha\beta n_0 - 4D/\lambda_0^2)$. The condition for growth is reminiscent of a Rayleigh-number criterion, with the gyrotactic length $\beta$ replacing a geometric dimension. When

$$\tau_d/\tau_g = \tfrac{1}{4}G = \frac{\alpha\beta\lambda_0^2 n_0}{4D} = \frac{(\Delta\rho/\bar{\rho})\, g\nu n_0 \beta\lambda_0^2}{4D\nu} > 1,$$

the perturbation grows. $\tau_d$ and $\tau_g$ are the time constants for diffusive decay and gyrotactic growth or recruitment. For the value of $G$ given in table 1, the perturbation grows when $\lambda_0^2 > 4/250 = 1.6 \times 10^{-2}$ cm$^2$. This value seems appropriate, considering experimental observations. When diffusion is negligible, the growth rate is given by $\alpha\beta n_0 = 1/\tau_g \approx 1/10\ \mathrm{s}^{-1}$, according to table 1. this rate is probably too rapid by approximately a factor of 2. It is, in any case, hard to observe because of extraneous perturbing factors, such as fluid motion remaining from earlier mixing (Kessler 1985*b*).

No attempt has been made to find decaying fluctuations for small $n_0$. It is difficult directly to observe cells at low concentration, and it has been found that flow-visualization techniques that use inert particles tend to modify cell behaviour.

## 6. Discussion and conclusions

Gravitational and viscous torques determine the average orientation of the trajectories of some swimming micro-organisms, such as single algal cells. As a result, algae that are suspended in a downward cylindrical Poiseuille flow swim toward its

axis. They swim toward the periphery in an upward flow. Cell separation techniques can be based on this phenomenon (Kessler 1986). It may also have significance in the non-uniform distribution of phytoplankton, a phenomenon which is frequently observed in nature.

Collective phenomena arise because of gyrotactic cell guidance, and because the cells are heavier than their suspending fluid. Cells accumulate in downflows owing to their interaction with gradients of the fluid velocity, whilst locally high cell concentrations generate downward buoyant convection of the concentrated region, at a rate that is generally higher than the cell's swimming speed. Because their centres of gravity are displaced rearward, individual cells tend to swim up in still water and transversely from ascending into descending regions of fluid. Thus the upswimming of individual cells is the cause of collective descent.

The dependence of collective phenomena on height and azimuth can be neglected in many experimental situations. With this assumption, and for small or zero self-consistently generated pressure gradients, a steady-state radial solution of the fluid momentum and cell conservation equations has been found. This solution provides a measure of the periodic spacing of gyrotactic concentration/convection patterns. It also provides a novel criterion for transition to time-varying behaviour. Circumstantial evidence suggests that the previously described (Kessler 1985*b*) blip instability is connected with that transition. Since the steady-state theory given in this paper avoids any consideration of $z$- and $t$-dependence, nothing further can be said about the generation of the blips. The theory simply states that when $n_0 \gamma R^2 \rightarrow 1$, the concentration profile collapses to a singularity, and when $n_0 \gamma R^2 > 1$, the $(t, z)$-independent treatment becomes invalid. It may be that when gyrotaxis is included in the treatment of Childress *et al.* (1975), their type of analysis may shed further light on the effect.

It is also rather surprising that (Childress & Percus 1981; Childress 1984) the chemotaxis of slime-mold amoebae is governed by equations similar to the ones presented in this paper, with $w(r, t)$ replaced by the concentration of a chemo-attractant. These authors also found that the cell system collapses toward the axis when a threshold analogous to $n_0 \gamma R^2 \rightarrow 1$ is exceeded. It may be that this type of collapse is not unusual for interacting populations of cells. In that case is could be a basic component of biological self-organization.

Some additional insight into the origin of the transition criterion may be gained by noting that (18) is the solution of

$$\frac{\mathrm{d}n(0)}{\mathrm{d}R_1^2} = [\gamma n(0)]\, n(0), \tag{33}$$

with $n(0)_{R_1^2=0} = n_1$. Equation (33) bypasses the previously given, more complex and explicit mathematical development. It assumes that the spatial accumulation rate $\gamma n(0)$ is proportional to the concentration. Equation (33) clearly demonstrates the limited cell-holding capacity of the gyrotactically concentrated column. The condition $n(0)_{R_1^2=0} = n_1$ means that when the accumulation radius is zero, the cell concentration everywhere remains at its average value.

The growth rate of a positive concentration fluctuation and the spacing of gyrotactic concentration/convection patterns were both found to be governed by a Rayleigh-number-like parameter $G = n_0 \gamma \lambda^2$. For the growth rate $\lambda = \lambda_0$ is the initial width of the fluctuation. For patterns $\lambda = R_1$, the pattern spacing. The gyrotaxis-characterizing constant $\beta$, which is contained in $\gamma$, is the third length in $G$.

Much additional work is required. Gyrotaxis of ellipsoidal cells embedded in a fluid

with vorticity and strain is being investigated with T. J. Pedley. The complete set of equations without suppression of $(\phi, z)$ remains to be solved. Experiments that will, hopefully, yield more definitive values of $D$ are underway. It is also necessary to ascertain whether the autorotation of the cells (Nultsch 1983) has any substantial effect. Finally, the question of the combination of taxes (e.g. light plus gyrotaxis), which leads to radical changes in pattern symmetry (Kessler 1986), remains wide open.

I should like to thank T. J. Pedley for a series of illuminating discussions which resulted in improvements, including the removal of an error from the original manuscript and the use of Bessel functions for treating the growth of cell concentration. I should also like to thank N. A. Hill for several important suggestions, the National Science Foundation, which supported attendance at the Symposium, and NSF Grant INT 85-13696.

## REFERENCES

CHILDRESS, S. 1984 Chemotactic collapse in two dimensions. In *Modelling of Patterns in Space and Time* (ed. W. Jäger & J. D. Murray), Lecture Notes in Biomathematics, Vol. 55, p. 61. Springer.

CHILDRESS, S., LEVANDOWSKY, M. & SPIEGEL, E. A. 1975 Pattern formation in a suspension of swimming microorganisms. *J. Fluid Mech.* **69**, 591.

CHILDRESS, S. & PERCUS, J. K. 1981 Nonlinear aspects of chemotaxis. *Math. Biosci.* **56**, 217.

DIEHN, B., FEINLEIB, M., HAUPT, W., HILDEBRAND, W., LENCI, F. & NULTSCH, W. 1977 Terminology of behavioral responses of motile microorganisms. *Photochem. Photobiol.* **26**, 559.

HAPPEL, J. & BRENNER, H. 1965 *Low Reynolds Number Hydrodynamics.* Prentice Hall.

JOSEPH, D. D. & LUNDGREN, T. S. 1973 Quasilinear Dirichlet problems driven by positive sources. *Arch. Rat. Mech. Anal.* **49**, 241.

KESSLER, J. O. 1984 Gyrotactic buoyant convection and spontaneous pattern formation in algal cell cultures. In *Nonequilibrium Phenomena in Physics and Related Fields* (ed. M. G. Velarde), p. 241. Plenum.

KESSLER, J. O. 1985*a* Hydrodynamic focusing of motile algal cells. *Nature* **313**, 218.

KESSLER, J. O. 1985*b* Cooperative and concentrative phenomena of swimming micro-organisms. *Comtemp. Phys.* **26**, 147.

KESSLER, J. O. 1986 The external dynamics of swimming micro-organisms. In *Progress in Phycological Research*, vol. 4 (ed. F. E. Round), p. 257. Bristol: Biopress.

NULTSCH, W. 1983 Photocontrol of movement of *Chlamydomonas*. In *The Biology of Photoreception* (ed. D. J. Cosens & D. Vince-Prue), p. 521. Soc. for Experimental Biology Symposium XXXVI.

ROBERTS, A. M. 1981 Hydrodynamics of Protozoan swimming. In *Biochemistry and Physiology of Protozoa*, vol. 4, 2nd edn (ed. M. Levandowsky and S. Hutner), p. 5. Academic.

TAYLOR, G. I. 1951 Analysis of the swimming of microscopic organisms. *Proc. R. Soc. Lond* A **209**, 447.

TAYLOR, G. I. 1953 Dispersion of soluble matter in solvent flowing slowly through a tube. *Proc. R. Soc. Lond.* A **219**, 186.